Elemental composition of grass phytoliths: Environmental control and effect on dissolution

Oleg S Pokrovsky, Alisson Akerman, Fabrice Fraysse, Marina V Olonova, Alexander A Kuznetzov, Sergey V Loiko, Jean-Dominique Meunier

Elemental composition of grass phytoliths: environmental control and effect on dissolution

Oleg S. Pokrovsky[1,2*], Alisson Akerman[1], Fabrice Fraysse[3], Marina V. Olonova[2], Alexander A. Kuznetzov[2], Sergey V. Loiko[2], Jean-Dominique Meunier[4]

[1] *Geoscience and Environment Toulouse, UMR 5563 CNRS, university of Toulouse, 14 Avenue Edouard Belin, 31400 Toulouse, France.*
[2] *BIO-GEO-CLIM Laboratory, Tomsk State University, Lenin Ave, 36, Tomsk, 634050, Russia*
[3] *Université de Lorraine, LIEC-Ecole Nationale Supérieure de Géologie, 15 Avenue du Charmois, 54500 Vandœuvre-lès-Nancy, France.*
[4] *CEREGE, Europôle méditerranéen de l'Arbois, BP 80, 13545 Aix-en-Provence, France.*

Keywords: *phytoliths, grass, silica, trace elements, dissolution*

Submitted to *Science of the Total Environment*

Corresponding author: oleg.pokrovsky@get.omp.eu

Abstract

Plant phytoliths, which represent the main pool of silica (Si) in the form of hydrous Si oxide, are capable of providing valuable information on different aspect of environmental issues including paleo-environmental reconstruction and agricultural sustainability. Phytoliths may have different chemical composition which in turn affects their preservation in soils ad impacts terrestrial cycle of the occluded elements including micro-nutrients and environmental toxicants. Yet, in contrast to sizable work devoted to phytoliths formation, dissolution and physico-chemical properties, the mechanisms that control total (major and trace) elemental composition remains poorly known. Towards assessing full elemental composition of phytoliths from different plants, here we measured 45 major and trace elements in 9 samples of grasses collected in northern Eurasia during different seasons, 18 grasses from Siberian regions, and 4 typical Si-concentrating plants (horsetail, larch, elm and tree fern).

In the European grasses, the variations of phytolith chemical composition among species were highly superior to the variations across vegetative season. Compared to European samples, Siberian grass phytoliths were impoverished in Ca and Sr, exhibited similar concentrations of Li, B, Na, Mg, K, V, Zn, Ni, Mo, As, Ba, and U, and were strongly enriched (x 100-1000) in lithogenic elements (trivalent and tetravalent hydrolysates), P, Mn, Fe and divalent metals. Overall, the variations in elemental composition between different species of the same region were lower compared to variations of the same species from distant regions.

The main factors controlling phytoliths elemental composition are the far-range atmospheric (dust) transfer, climatic conditions (humidity), and, in a lesser degree, local lithology and anthropogenic pollution. Despite significant, up to 3 orders of magnitude, difference in TE composition of grass and other plant phytoliths, the dissolution rates of grass phytoliths measured in this study were similar, within the experimental uncertainty, to those of other plants studied in former works. Therefore, elemental composition of phytoliths has relatively minor impact on their preservation in soils.

1. INTRODUCTION

High importance of the biogenic cycle of silicon in terrestrial environments has been widely recognized (Meunier and al., 1999; Conley, 2002; Derry and al, 2005). Dissolved silicic acid, trapped by plant roots, precipitates in aerial tissues cells as micrometric opal particles called phytoliths (Neethirajan et al., 2009; Guerriero et al., 2016; Hodson et al., 2016). Studies on phytoliths have shown applications in various environment fields linked to ecosystems services (Meunier et al., 2022; Hussain et al., 2023). Phytoliths are released during organic matter degradation in the litter horizon and can be dissolved, preserved and transferred to deeper horizons, or evacuated by aerial or hydrographical ways (Bartoli, 1981; Piperno, 1988; Kaczorek et al., 2019). The dissolved (water-labile) fraction constitutes a pool of Si that is easily available for plants (Shaller et al., 2019). Silicon bioavailability is a topic of increasing interest because of the positive impact of Si on sustainable agriculture (Liang et al., 2015). The fraction that is preserved from dissolution can be used as a proxy for palaeoenvironments (Cabanes, 2020). Understanding the reactivity of phytolith is therefore essential for predicting the behaviour of phytoliths in the environment.

Experimental studies on the dissolution rate of natural phytoliths demonstrated their similarity to quartz and amorphous silica, with a minimum in acidic solutions and in increase in dissolution rate with pH in neutral and alkaline solutions (Fraysse et al., 2006 a, b; 2009; 2010). However, while the reactivity of phytoliths is relatively well characterized, it is not so for their elemental composition and the role that incorporated metals exert on phytoliths dissolution behaviour. Besides Si, some major and trace elements can be trapped in phytoliths (Hodson, 2015) but their effects of phytolith reactivity as well as their role in tracing soil and plant type remain poorly assessed. Carbon trapped in phytoliths has been first measured by Jones and Beavers (1963) which is widely used in the field of phytolith dating and carbon sequestration (Santos et al., 2012; Li et al., 2013; Hodson, 2018). Nguyen et al (2015) showed

that potassium (K) incorporated into phytoliths might affect the fertility of soils. Aluminium (Al) is also occluded in phytoliths but the effect of Al on phytolith reactivity is controversial (Fraysse et al., 2009; Li et al., 2014). Carnelli et al (2002) found that woody taxa contain higher concentration of Al suggesting applications in paleo-vegetation studies. Metals such as Cu and Zn have been shown to be encapsulated in phytoliths with consequences for their terrestrial biogeochemical cycles (Nguyen et al., 2019; Tran et al., 2019). A few studies have tested the hypothesis that the composition of multi-elements in phytoliths might be used for tracing of environmental conditions (Cabanes, 2020; Hart, 2001; Li et al., 2020; Tan et al., 2022). Thus, elemental composition of wheat and barley phytoliths has been reported to be strongly sensitive to contaminations on the surface of the leaves and awns (Kamenik et al., 2013; Wyttenbach et al., 2002; Kucera et al., 2007). In particular, Kameník et al. (2013) measured 30 major and trace elements in barley's phytoliths and provided the relationship between phytoliths composition and that of source plant materials demonstrating that phytoliths are significantly enriched in terrigenous elements. Two studies characterized the distribution of multiple trace elements (Al, Fe, Mn, Cu, Zn, Cr, Ni, Pb, As, Sn, Cd) in grass and shrub phytoliths within a mining contamination context (Bujan et al., 2013; Delplace et al., 2020). The latter authors demonstrated strong encapsulation in siliceous matrix of As, Cu, Mn, Pb and Zn, in contrast to Cd, Sb and Sn which were prone to be concentrated in organic biomass. However, up to present time, the variations of elemental composition of the same plant from different geographic regions, non-affected by specific local pollution source, remain largely unknown. This does not allow incorporating the role of phytoliths in overall biogeochemical cycle of trace element in terrestrial plants. The first goal of the present study was a first-time assessment of large number (about 50) of major and trace elements in phytoliths of typical grasses (Poaceae) of Northern Eurasia, across seasons and geographical locations. We further compared the elemental composition of grass phytoliths to that of other plants known to concentrate Si in their tissues

(horsetail, fern, larch, elm; Fraysse et al., 2009). Via normalization to average earth crust composition, we intended to assess elements that are preferentially enriched in phytoliths in order to provide some insights into the biological (active or passive) concentration mechanisms.

Our second goal was to quantify the dissolution kinetics of previously unknown grass phytoliths, and compare the rates with those already available for other plants. Here we intended to relate the difference in elemental composition between different plants to phytoliths reactivity (dissolution rates) in aqueous solutions. Taken together, the present study should improve our capacity to use phytoliths for tracing TE migration in soil system and to relate the phytoliths preservation ability in soil to their elemental composition.

2. MATERIALS AND METHODS

2.1 Study sites and collected plants

Five plant species growing on different soil, under various climatic conditions and containing phytoliths have been investigated. The grass phytoliths belong to the same plant family, *Poaceae* (formerly known as Graminae) are listed in the **Table 1**, and include wood small-reed (*Calamagrostis epigejos*), rough small-reed (*Calamagrostis arundinacea*), reed-mannagrass (*Glyceria maxima*), sweet vernal grass (*Anthoxanthum odoratum*) and common reed (*Phragmites communis*). Included in this table also the climate parameters of the sampling site, type of soil and its mineral substrate. The European grasses (samples E1 to E11) were sampled in the boreal zone of Eastern Europe, between 1998 and 2003 during summer period (June to August). This collection allowed testing 1) the variability of elemental composition among several species (*P. communis*, *G. maxima*, *C. arundinacea* and *C. epigejos*), which were sampled during the same period in the same place (West Dvina, July-August 1998); 2) the effect of growth stage (beginning of June and end of June) for the same specie (*C. epigejos*) collected

131 in the same place, and 3) the variability of phytolith elemental composition of the same specie
132 (*C. epigejos*) collected across different regions.

133 The grasses from Siberia were obtained from Krylov's botanical collection of the Tomsk
134 State University and included *P. communis*, *C. arundinacea*, *C. epigejos*, *A. odoratum*, and *G.*
135 *maxima*. These samples were collected during July-August period, and included northern taiga,
136 forest-steppe and steppe biomes (between 51.4 °N and 62.0 °N) in the Krasnoyarsk, Omsk,
137 Tomsk, and Novosibirsk administrative regions, Baraba, Tuva, Buryatia, Altai, Yakutia (**Fig.**
138 **1**, **Table 1**). Grass phytoliths in this study are compared to phytoliths of horsetail (*Equisetum*
139 *arvense*), larch (*Larix gmelinii*), elm (*Ulmus laevis* Pall.), and tree fern (*Dicksonia squarrosa*)
140 that are known to concentrate Si in their biomass (Fraysse et al., 2009).

141

142 *2.2. Phytoliths extraction*

143 All the manipulation were performed in a clean room class A10,000. Transferring solid,
144 solutions, and addition of chemicals was performed in the laminar hood box class A100. First,
145 dry plant material (10-20 g) was rinsed by Milli-Q ultrapure water, and then dried in an oven at
146 50°C. Afterwards, it was ground in an agate mill. Ashing of plant material was performed in a
147 porcelain crucible at 500°C for 8 hours. Note that calcination at 500 °C gives the best results
148 for phytolith extraction (e.g., Bujan, 2013). The ash (approximately 0.2 g) was then transferred
149 to polypropylene tubes, into which we added 10 mL of 10% ultra-pure bidistilled HCl to
150 dissolve all insoluble solid phase except silicon oxide. The content was heated in the water bath
151 at 70°C during 20 min, and then centrifuged at 3500 rpm for 5 min followed by decantation. To
152 remove the last traces of organic matter, we added 10 mL of ultra-pure 15% H_2O_2 and heated
153 the content in the water bath at 70°C during 20 min. Finally, the residual solid material was
154 rinsed with Milli-Q water via repetitive centrifugation at 3500 ppm during 20 min, and dried at
155 50°C during 48 hrs in an oven. The cleaned phytoliths were examined by scanning electron

156 microscopy (SEM) using a Jeol JSM840a, coupled with a SDD PGT Sahara EDS analyzer in
157 order to check the lack of contaminants and identify different morphotypes.

158 Phytoliths were extracted from plant material by dry ashing which is most efficient way
159 to remove organic matter (Parr et al., 2001a, b). These authors demonstrated that morphological
160 pattern of phytoliths (dimensions and curvatures) obtained via dry ashing (500 °C) and wet
161 (boiling) extractions are statistically identical. The dry ashing method of phytolith extraction
162 used in this study is not expected to produce any artefacts of preparation. Indeed, the electronic
163 microscopic observations of freshly extracted and reacted phytoliths did not reveal any heat-
164 generated smoothing and melting features on the surface. The X-ray diffraction analysis of our
165 phytoliths material did not demonstrate the presence of any crystalline phases. Moreover, a
166 thorough methodological work of Parr et al. (2001) demonstrated that phytoliths pattern
167 dimensions and curvatures preparations via dry (500°C) and wet (boiling) are statistically
168 identical and there is no detectable evidence of morphological impact as a result of these
169 methods. Recent results of Delplace et al. (2020) on grass phytoliths demonstrated a lack of
170 artefacts linked to organic matter presence in phytoliths which allows adequate assessment of
171 elemental composition of phytoliths prepared via dry ashing. At the same time, we do not
172 exclude some redistribution of metals (i.e., Zn) from the organic material to the silica, possibly
173 promoted by the release of structural water from amorphous opal throughout the heating
174 procedure at higher temperatures (i.e., at 700 °C; Sarret et al., 2022).

175 Further, we have to admit that there is no possibility of separating the phytoliths from
176 refractory silicate minerals which are insoluble in concentrated HCl at the stage of phytolith
177 extraction as described above. While these minerals are unlikely to be incorporated inside the
178 plant biomass, adventitious dust of atmospheric aerosols can be attached to the leaf surfaces
179 and not removed even after thorough water rinsing. Although the amount of these minerals is
180 negligible, given lack of their identification by XRD and SEM, they still are capable of

accommodating some trace elements which are unrelated to phytoliths per se. Use of refractory elements without any physiological functions (Al, Ti, Zr), when interpreting the elemental phytoliths after total acid leaching (see section 2.2 below), can help to resolve these possible artefacts.

2.3 Analytical methods

For total Si content in the phytoliths, powdered sample (between 10 and 20 mg) was entirely digested in 10 ml of 30% NaOH at 120°C during 2 h in closed Savillex Teflon vials, then treated in ultrasonic bath for 2 h and heated again at 120°C overnight. The solution was centrifuged and 1 ml of supernatant was then diluted in 10 ml of ultrapure deionized water and acidified with bi-distilled HCl 10 N in a 1/1 (molar/molar) ratio. Total silica concentration in phytoliths was measured using the molybdate blue method with High Resolution Digital Colorimeter (Bran + Luebbe Auto-analyser III using control software AACE 6.03) with an uncertainty better than 2% and a detection limit of 0.36 µM.

The mineralization of phytolith sample (between 15 and 30 mg) involved 0.5 ml of Suprapur HF and 0.6 ml of bi-distilled 15 N HNO_3 which were added together in closed Teflon vials in a class 10,000 clean room at the GET laboratory (Géoscience Environnement Toulouse, France). The Teflon vials were heated on a hotplate located inside a polycarbonate chamber (class A100 filtered air). International certified materials (2711a Montana II Soil standard or LKSD sediment) were processed together with samples to account for accuracy of measurements. Besides, the international geostandards of Apple Leaves SRM 1515(from NIST, USA), lichens BCR-CRM 482 (from BCR, Belgium), and Pine Needles SRM 1575a (from NIST, USA) were used to check the efficiency of both the acid digestion protocol and the analysis.

Major and trace elements concentrations in phytoliths were obtained via quadrupole ICP-MS (inductively coupled plasma mass spectrometry, Thermo Scientific) at HSM laboratory (HydroScience Montpellier, France) and GET Laboratory (Toulouse). To each sample, ~3 µg/L of In and Re were added as internal standards. Four in-house external standards were analysed every 10 samples. The uncertainty for TE measurement ranged from 5 % at 0.1–100 µg/L to 10 % at 0.001–0.01 µg/L. The data tables present results for elements exhibiting a good agreement between the certified or recommended values and our measurements (relative difference expressed as $([X]_{recommended\ or\ certified} - [X]_{measured})/(([X]_{recommended\ or\ certified} + [X]_{measured})/2)*100$ lower than 10 %), or for cases where we obtain a good reproducibility (relative standard deviation on our various measurements of standards lower than 10 %), even if no certified or recommended data are available.

Blank tests indicated that the level of contamination induced by the acid digestion procedure was negligible, < 2% of the sample element of interest. The international geostandard SLRS-5 (Riverine Water Reference Material for Trace Metals certified by the National Research Council of Canada) was used to check the validity and reproducibility of solution analyses.

2.4. Phytolith reactivity in aqueous solution

Phytoliths dissolution rates were measured in batch reactors at 25°C in 0.01 M NaCl solution. Phytoliths suspensions of 2.5 g/L were prepared in 100 mL polypropylene reactors and dissolution rates were calculated by measuring dissolved silica concentration as a function of time. The reactors were agitated on a Ping-Pong shaker (150 rpm). Typically, between 10 and 20 samplings were performed over elapsed time between 3 and 4 hrs. About 5 mL of suspension was sampled under vigorous stirring, without changing the solid : solution ratio in

the reactor; the fluid was filtered through 0.22 μm acetate cellulose filter and stored in the refrigerator pending spectrophotometric analysis of Si.

The dissolution rate of phytoliths (R, mol Si g^{-1} d^{-1}) was calculated from the slope of Si concentration vs elapsed time (d[Si]/dt) following the equation:

$$R = \frac{d[Si]}{dt} \times \frac{1}{m}$$

where m is the concentration of phytoliths in the reactor. Solution pH was measured using a combination glass electrode (Mettler Toledo) calibrated with NIST buffers (pH 4.01, 6.86, 10.00 at 25°C), with an uncertainty of 0.01 pH units.

2.5. Data treatment

Statistical treatment of the data included mean values and their standard deviations (in case of replicates and for calculating the mean concentrations of several species. Pairwise (Pearson) correlations were used to assess the relationship between major and trace elements in phytoliths, separately for European, Siberian grasses and other plants, as well as for the full set of data. Further, a pairwise comparative analysis was run via non-parametric Mann-Whitney test (U-test) to detect the differences in elemental composition of various species and the same species from different locations, as well as between Si release rate from different phytoliths. The level of significance was fixed at 0.05 (95% confidence level) to consider a result as statistically notable. All plots were built using MS Excel 2016 and the Statistica-12 software package (http://www.statsoft.com).

3. RESULTS AND DISCUSSION

3.1 Phytolith morphology, total Si content in phytoliths and phytoliths's content in the biomass

The phytoliths preparation procedure employed in the present study yielded clean

particles of various size and forms without visible admixture of crystalline silicate minerals or metal oxides, as also confirmed by EDX analyses of selected spots of the samples (**Fig. S1**). The presence of organic residues could not be established by a thorough SEM examination. Similar to former studies of phytoliths from soils (e.g., Kaczorek et al., 2019), several main morphotypes were identified, such as globular, elongated, vascular, plain, porous, and cratered/spongy. We could not detect clear difference in bulk chemical composition (Si, O, C, Al, Fe, Ca) of phytoliths of different morphotypes via EDX probing (not shown). Although some differences in elemental composition of different phytoliths could be present (e.g., Kaczorek et al., 2019), we used sizable amount of homogenized (pooled) phytolith particles from each plant for total acid leaching. As such, we integrated several phytolith morphotypes for each analysis and the obtained data for each species and each location can be considered as integral values incorporating large number (> 20) of individual phytoliths.

Phytoliths content in the biomass ranged from 0.9 to 6.7% and 0.2 to 3.1% in European and Siberian grasses, respectively (**Table 2**). This is similar to the values in trees (3.4 and 3.8 in larch and elm, respectively) but lower than that in typical Si-concentration plants such as fern and horsetail (12 and 14 %, respectively). Other studies reported 1-3 % in dryland grasses and up to 10-15% in some wetland plant species (Epstein, 1994), with a general range for plants of < 0.1 to 10% Si in shoot dry matter (Epstein, 1999). Bujan (2013) reported the range of phytolith content in Ericaceae leaves from 0.5 % in organic soils to 2.5 % in mine and serpentine soils.

The total Si concentration was quite similar in all phytoliths from Europe and ranged from 1.26 to 1.52 × 10^{-2} $mol_{Si}.g^{-1}_{phytoliths}$. By considering an average of (1.40 ± 0.01)×10^{-2} $mol_{Si}.g^{-1}_{phytoliths}$ for the $[Si]_{total}$ in phytoliths, this suggests 39.3 mass % of Si in phytoliths which is in accord with Blecker et al. (2006) who estimated a value of 39.7% for Si content in phytoliths of various plants. The phytoliths from Siberian plants exhibited much higher variability of Si content (from 15.6 to 57.3 %), with an average value of 33.7±10.1 %. Assuming

a phytolith formulae of $SiO_2 \times nH_2O$, this corresponds n = 0.62 to 1.28 (average 0.95), and suggests, in accord with previous results (Fraysse et al., 2009), that phytoliths of different plant species have similar major composition.

3.2. Phytoliths of European grasses: variations among species and across seasons and sites.

The variability of trace element (TE) composition of the same grass species from different geographical (climate) zones were weakly pronounced, thus suggesting that element concentration in phytoliths is their intrinsic, species-related property. Phytoliths chemical compositions of different plant species sampled at the same time (July-August 1998) from the same place (West Dvina, Russia) could be compared among samples E4, E7, E11 and E5 corresponding to *Phragmites communis*, *Glyceria maxima*, *Calamagrostis arundinacea* and *Calamagrostis epigejos* (**Fig. S2)**. One can note general similarity of elemental composition with highest concentrations of Mg, Ca, Mn, Fe, Zn, Sr, Mo, Ba and U in all samples.

After normalization of phytolith composition to that of the upper crust (Rudnick et al., 2004), an enrichment in Mg, Ca, and Sr appears (ratio phytoliths : crust > 1, **Fig. S3**). The crust-normalized rare earth elements (REE) patterns of phytoliths from different species are highly variable with exceptional Eu enrichment of *C. epigejos* and *P. communis* and generally flat pattern for other species (**Fig. S4**). Another comparison, for the same species sampled during different vegetation period could be performed for samples E3 and E10 of *Calamagrostis epigejos* from Yaroslavsk region (European Russia). There was no sizable difference in major and trace element concentrations between these samples (**Fig. S5**).

Finally, the variations in elemental composition of phytoliths extracted from *Calamagrostis epigeios* which was sampled during summer in different regions of Eastern Europe, also demonstrated general similarity among sites, with highest concentration of Ca,

Mg, K, Sr, Ba, Fe, Mn, Zn, Ni, As, Mo and U (**Fig. S6**). An upper crust (UC) – normalized pattern demonstrated slight enrichment of phytolith in Ca, and Sr and similarity of concentrations in phytoliths and UC of Mg, Ga, As, and Mo (**Fig. S7**). All samples of *Calamagrostis e.* exhibited an enrichment in HREE relative to LREE and a local Eu maximum (**Fig. S8**).

Taken together, phytoliths of European grasses were rather similar among species (**Table S1; Fig. 2A**), whereas, compared to UCC, their elemental pattern was similar in concentrations of B, Na, Mg, Si, and Mo, strongly enriched in Ca, Se and Sr, and strongly (x 10^3-10^4) depleted in lithogenic trivalent and tetravalent trace elements and divalent metals (**Fig. 2B**).

3.3. Elemental pattern of phytoliths from Siberian grasses

The phytoliths from Siberian grasses exhibited distinct difference in their elemental composition from phytoliths of European Russia (**Fig. 3 and Fig. S9**). Siberian phytoliths were strongly (x 10^2-10^3) enriched in most lithogenic elements (Al, Ti, Cr, Y, Zr, Nb, REEs, Hf, Th) but also macro- and micro-nutrients (P, Mn, Fe, Co, Ni, Cu, Zn, Rb), Cs and some trace toxicants (Cd, Tl, Pb). At the same time, phytoliths from European grasses (*Phragmites, Calamagrostis*) were sizably (> × 10) enriched in Ca, Sr and Se, and exhibited comparable concentrations of Li, B, Na, K, Mg, V, Zn, As, Mo, Ba and U.

Alike European samples, Siberian phytoliths had rather similar concentrations of all major and trace elements across four studied species (**Fig. 3A**). The difference between species was similar or inferior to the variation in elemental composition within the same species. The latter typically achieved a factor of 2 to 3, although for phytoliths of *Calamagrostis epigejos*, this difference for many elements reached a factor of 5 (**Table S2**). Although the upper crust – normalized patterns of major and trace elements in Siberian phytoliths were globally similar

among different species (**Fig. 3B**), we noted that, compared to other species, phytoliths of *Anthoxanthum* were distinctly enriched in essentially lithogenic low mobile elements such as Ti, V, Cr, Fe, Co, Y, Zr, Nb, REEs, Hf, Ta, Th and U. We could not detect distinct differences in elemental concentrations of phytoliths from different locations, having different soils and highly contrasting climate (including most remote Yakutian sample S1 of the permafrost zone and sample S18 from frozen peatlands of Western Siberia). Similar conclusion has been achieved for samples of the same grass species collected during different years in neighbouring settings (S10 and S4; S5 and S9 of Krasnoyask and Tomsk regions).

Much higher concentration of insoluble (low mobile, lithogenic) elements in Siberian phytoliths could be partially linked to higher aridity of the climate, hotter vegetation period and generally stronger evaporation, compared to the European part of Russia. These conditions are likely to facilitate the retention of metals within the plants. At the same time, we have not evidenced a correlation between given element concentration and mean annual precipitation (MAP) ($p > 0.05$). For example, the samples collected from the sites of lowest MAP (300-350 mm y^{-1}), E6 in Europe and S2, S8, S14 and S16 in Siberia, did not exhibit particularly high metal concentration, compared to phytoliths from other sites of two territories. An enrichment of phytoliths from European grasses (*Phragmites, Calamagrostis*) in Ca and Sr could be linked to dominantly carbonate rocks and sedimentary silicate as lithological substrate for soils developed in this part of the Russian Platform, compared to the Siberian Platform and mountain regions, where the dominant soils are developed on crystalline silicate rocks.

3.4. Comparison of phytoliths from grasses and other plants (horsetail, larch, tree fern and elm)

Earlier works demonstrated that grass (bamboo) phytoliths are rich in K, Mg, Na and Ca, whereas phytoliths from woody species are enriched in lithogenic elements (Al, Sc, Ti, V,

354 Cs, Fe, REE) because they contain higher proportions of aluminosilicates (Jones et al., 1966;
355 Carnelli et al., 2002; Kamenik et al., 2013). Results of the present study confirm these general
356 features while strongly extending the list of major and trace elements that exhibit different
357 behaviour in phytoliths from different grasses.

358 Combining both European and Siberian species (*C. epigejos*, *G. maxima*, *P. communis*,
359 *A. odoratum*, and *C. arundinacea*), the elemental composition of grass phytoliths (**Table 3**) can
360 be compared to that of other plants such as horsetail (*Equisetum arvense)*, larch (*Larix*
361 *gmelinii*), elm (*Ulmus laevis Pall.*) and tree fern (*Dicksonia squarrosa*) as illustrated in **Fig. 4**.
362 Compared to phytoliths of *E. arvense*, *L. gmelinii*, *U. laevis Pall.*, and *D. squarrosa* originated
363 from France, Siberia, Ukraine and New-Zealand, respectively, Eurasian grass phytoliths are
364 sizably enriched in Li, B, Na, Mg, Ca, Se and Sr. All other major and trace elements in grass
365 phytoliths exhibited concentrations that were within their variations among four other plant
366 species. Noteworthy that two plants that are known to concentrate Si most significantly
367 (horsetail and fern, having 14 and 12 % of phytoliths in their biomass, respectively) did not
368 exhibit any particulate elemental pattern compared to phytolith-poor grasses such as *P.*
369 *communis* (0.51 %, sample S15) or *A. odoratm* (0.16 %, sample S6) from Siberia.

370 The mean concentrations of B, Na, Si, P, Sr, Mo, Ag, Cd, and Sb in grass phytoliths are
371 comparable to those of the upper crust. At the same time, grass phytoliths are generally poor in
372 all lithogenic elements such as trivalent and tetravalent hydrolysates, divalent heavy metals, Ta,
373 Bi, W, U. Compared to phytoliths studied in other works, Eurasian grass phytoliths are
374 comparable in Mg and Ca concentrations to phytoliths of Ericaceae from Iberian Peninsula
375 (Bujan, 2013), but they are strongly, more than a factor of 10, impoverished in all metals (Al,
376 Fe, Mn, Cr, Ni, Zn, Cu, Pb) and As. There are several possible explanations for this difference.
377 First, Iberian metal belt is well-known for its high metal concentration in soils, hence the
378 capacity of Ericaceae's phytoliths to accumulate Fe, Mn, Cu, Zn, Pb and As at the level strongly

exceeding that observed in mine-free sites (Bujan, 2013). However, the phytoliths of Iberian grasses sampled from unpolluted soils (serpentinite, quartzite, and peat) also demonstrated more than an order of magnitude higher concentrations of all trace metals compared to Eurasian grasses. A second possible explanation is specificity of heathers (Eriaceae) metabolism that are capable to immobilize trace metals by Si in vacuoles of living cells or in the cell wall (e.g., Montes-Botella, 2001) therefore augmenting the tolerance of plants to metal pollutants (Rossini et al., 2009, 2011). A third possibility is rather pristine environment of Eastern European and Siberian sites where the grasses were collected. In the Russian Plain, the sites are remote from any centers of local industrial or domestic pollution, and rather far from aerosol dust provinces. The latter can deliver silicate material to the land surface, which then can be absorbed by plants. Siberian sites are closer to local desert or semi-desert regions that are known to be sources of solid aerosols (Kazakhstan, Mongolia), and this can explain an enrichment in many lithogenic elements of the Siberian grasses relative to the European part of Russia. The influence of atmospheric silicate deposition on the snow cover of southern regions of Western Siberia leading to an enrichment in lithogenic elements is fairly well established from Siberian snowpack studies (Shevchenko et al., 2017, 2020; Krickov et al., 2022).

The Sahara desert influence on Iberian sites of grass collections is much higher than the impact of far-range atmospheric transfer from deserts of Central Eurasia on Siberian sites, given the relative geographical distances. The industrial activity in the Iberian Peninsula is also much lower than that in Siberia. Note that the sampling in Siberia was performed 50 to 70 years earlier than that in Spain. As a result, many anthropogenically-impacted trace elements (Cu, Zn, Cr, Ni, Pb and As) could originate from local atmospheric fallouts (industry, roads, domestic emissions) and be pronounced in grasses from Spain. Enhanced uptake of trace element by plants from contaminated soils may also become the dominant mechanism of phytolith enrichment in trace pollutants. Thus, phytoliths of reeds growing in mining environments

(metal sulfide ores) of Southern Europe (e.g., Delplace et al., 2020) were strongly (> 10-100 times) enriched in Mn, Cu, Pb, Zn, As, Cd, Sb and Sn compared to grass phytoliths from pristine environments analyzed in the present study. Alleviating the toxicity of such pollutants via adsorption and coprecipitation with amorphous hydrated silica oxide, linked to intracellular phytoliths production, is well known for various plants of the world (Turnau et al., 2007; Keller et al., 2015; Rizwan et al., 2016; Delplace et al., 2020; Liu et al., 2022, 2023; Sarret et al., 2022). However, we admit that a new contemporary sampling of Siberian grasses is necessary to judge the level of anthropogenic pollution and its impact on chemical composition of grass phytoliths.

Finally, alike for the local difference between European grasses growing in more humid climate compared to Siberian grasses of dryer and hotter summer periods, the global difference between Eurasian and Iberian phytoliths may reflect hot and dry climatic conditions of the latter, given that the temperature and precipitation are among the primary factors that control the size, localization and shape of phytoliths from common reed (e.g., Liu et al., 2016 a, b). Under dry Iberian climate and lack of water during grass maturation period (end of summer), the immobilization of even soluble metals inside the tissue and within the phytoliths may become quite efficient. This hypothesis, however, requires further verification by both natural observations and laboratory-scale experiments.

In addition to the source control described above, soil pH might be a non-negligible factor of insoluble element enrichment in phytoliths. Thus, Hodson and Sangster (1999) demonstrated that, for Al in conifers, free Al is mobilized in soils affected by acidic precipitation; this Al is then taken up by plants and sequestered in phytoliths. However, we could not evidence any relationship between soil water pH (estimated for the sampled sites from soil typification) and insoluble element concentration in phytoliths (not shown). Therefore, it remains unclear, to which degree the other trivalent and tetravalent elements, typically more

labile in acidic environments, are capable to follow the Al pathway through the atmospheric precipitation, soil migration and plant phytolith accumulation.

3.5. Elemental correlations in phytoliths and mechanisms of elemental uptake

Pairwise (Pearson) correlation coefficients (**Table S3**) demonstrated two main groups of major and trace elements, present in both Eurasian and Siberian phytoliths. Labile elements (alkali and alkaline-earth metals), B, Mo, Se, but also Cu and Zn exhibited significant ($0.5 < R_{Pearson} \leq 0.98$; $p < 0.01$) correlation with Na and Ca as major indicators of such soluble elements. The second large group of inter-correlated components was constituted of lithogenic elements and included trivalent (Al, Fe, Y, REEs), and tetravalent hydrolysates (Ti, Zr, Hf, Th), Cr, V, Mn, Co, Nb, Tl, Bi, Pb. It is important to note that As correlated with both Fe and Al in the Siberian phytoliths, whereas P correlated only with Al. We therefore hypothesize an overwhelming role of Fe and Al hydroxides as carriers of many insoluble trace elements as well as some major (P) and micro- (V, Co, Ni) nutrients in grass phytoliths. These TE^{3+}, TE^{4+} -bearing oxy(hydr)oxides could be dispersed (occluded) within the bulk of the phytoliths rather than being adsorbed the phytolith surface, given that the phytoliths were treated with HCl during their extraction. This result corroborates former observations on phytoliths of barley that were enriched in several lithogenic elements (i.e., Al, Sc, Ti, V, Cs, and Fe), reflecting endogenous source of these elements (Carnelli et al., 2002).

We further believe that the two groups of inter-correlated elements described above reflect two main sources of material that is deposited onto plant leaves via atmospheric transfer. The two sources are known from atmospheric aerosols and snow precipitation studies in Siberia (Shevchenko et al., 2017; Krickov et al., 2021, 2022): 1) carbonate mineral particles, providing a signature of labile elements and 2) silicate and other refractory minerals, providing a signature

of lithogenic material. In addition, these two natural sources can be combined with atmospheric dust from local anthropogenic pollution (Zn, Cd, Pb, As).

The main element constituting plant phytoliths, after Si and O, is Ca. The primary cell wall contains around 35% of pectin, which is crosslinked by coordination with Ca ions (e.g., Perry and Keeling-Tucker, 1998). Presumably, during silica mineralization within the Ca-rich cell wall region, sizable amount of Ca can be taken up by / coprecipitated with amorphous hydrous Si oxide. Magnesium, Sr and Ba, also exhibiting high concentrations in phytoliths, could participate, together with Ca, in pectin cross-linking assemblages and hence enrich the forming Si phases. Sizable amount of Fe and Al in the phytoliths could be linked to strong capacity of both cations to maintain silicic acid in solution up to its solubility limit (Perry and Keeling-Tucker, 1998) thus playing some role in the genesis of the solid phase. Any information on other trace cations, likely to be (passively) present within the sites of silica deposition and can enter the phytoliths via co-precipitation with $Si(OH)_4$ (s), is currently not available. Elucidating these mechanisms requires specially designed in-vitro laboratory experiments.

Some trace elements, belonging to both 'labile' and 'insoluble' group of phytoliths' constituents described above and serving as micro-nutrients for plants (B, Zn, Mn, Ni, Co, Mo, Se) can enter the plant according to 'internal' metabolic requirements, regardless of availability of external soil stock. After being carried within the plant tissues via protein and carbohydrate components of the organic matrix associated with Si (e.g., Perry and Keeling-Tucker, 2000; Perry and Fraser, 1991; Currie and Perry, 2007; Belton et al., 2004, 2012), they eventually can be deposited within the cell interior in the form of coprecipitates with amorphous silica, which happens within cellular fluids and sap solutions. At the same time, TE interaction with silicon transporters involved in biosilicification in plants such as proline-rich proteins and siliplant_1 protein (e.g., Nawaz et al., 2019) remain virtually unknown. Strong control on TE fractionation during phytolith formation may be exerted by cell wall polymers complexation with trace

478 cations and anions, given that the polymeric template controls the shape and size of colloidal
479 Si particles as it is known for horsetail (e.g., Sapei et al., 2007). Note that both trace cations and
480 oxyanions can strongly interact with proteins and silica moieties of cell walls of diatoms
481 (Gélabert et al., 2018), similarly to what may occur in sites of plant phytolith deposition.

482 During these interactions, soluble, labile alkalis, alkaline-earth metals and oxyanions
483 exhibit a distinctly different behavior from low soluble, low mobile trivalent and tetravalent
484 hydrolysates. Note that in this discussion of element affinity to phytoliths and relevant
485 mechanisms, we ignore the diversity of phytoliths morphotypes, which can reflect different
486 sites and modes of amorphous silicate deposition in plant cellular structure (e.g., Nawaz et al.,
487 2019). It is possible that phytoliths of different shape, water and Si content and density, being
488 formed in different parts of grass leaves, have different elemental composition. Phytolith
489 morphotype-specific analyses via high spatial resolution laser ablation or nano-SIMS
490 techniques would be necessary to verify this possibility.

491

492 *3.6. Effect of metals (Fe, Al, Ca, Mg) on phytoliths dissolution kinetics*

493 Dissolution kinetics of *Calamagrostis epigejos* from Europe could be tested only for the
494 five samples of this specie, for which we possessed sufficient amount of phytolith material for
495 multiple batch experiments (**Table 4**). Individual experimental results are illustrated in **Fig.**
496 **S10**. In order to assess the effect of major element (Ca, Mg, Fe, and Al) concentration in
497 phytoliths on Si release rate, we first compared the concentration level of these elements in
498 grass phytoliths studied in this work to that previously assessed in horsetail, fern, larch and elm
499 (e.g., Fraysse et al., 2009). A histogram of major elemental composition of various phytoliths
500 (**Fig. 5**) illustrates that grass phytoliths are 100-1000 and 10-100 times lower in Al and Fe
501 concentration, respectively, and strongly (x 100 for Ca, x 10 for Mg) enriched in alkaline-earth
502 elements compared to other phytoliths. However, despite these sizable differences in elemental

composition of various phytoliths, all of them exhibited similar (±0.2-0.3 log *R* unit, which is within the experimental uncertainties) rates of Si release as shown in a plot of the log R_{Si} of phytoliths as a function of aqueous solution pH **(Fig. 6)**. This finding is also consistent with similarity (within ±0.35 log *R* unit) of silicate mineral dissolution rates in the circumneutral pH range as recently reported by Hermanska et al. (2023). In agreement with latter authors, we suggest that observed similarity in dissolution rates is due to the fact that these minerals, but also hydrous amorphous silica, are controlled by the breaking of the same, tetrahedral Si-O, bridging bonds. At these circum-neutral pH conditions, there is a limited exchange of divalent and trivalent cations (c.f. Oelkers, 2001; Oelkers et al., 2009) that are likely present within the amorphous hydrous silica. Therefore, because there is no sizable impact of breaking the bonds between metal and oxygen which are adjacent to Si-O bonds, the overall dissolution rates of phytoliths containing different proportion of Ca, Na, Fe and Al are weakly dependent on major elemental composition. It is of note that various soils also exhibit similar Si release rate in the circum-neutral solutions (Lim et al., 2023) which stems from the similarity of bond-breaking mechanisms for silicate minerals as described above.

A global significance of this result is that phytoliths' reactivity in aqueous solution, and hence, their preservation in soil horizons are weakly dependent on the concentration of major and trace element occluded within these phytoliths. This may justify the use of phytoliths for various paleo-reconstructions, as well as for tracing the external input of pollutants, plant metabolic requirements and detoxification mechanisms in case of anthropogenically-affected settings. At the same time, phytoliths are capable of Al adsorption (Bartoli 1985) and some studies have shown that soil phytoliths are more resistant to dissolution compared to fresh phytoliths (Liu et al., 2023). Such a resistance is commonly linked to chemisorbed Al (Van Cappelen et al., 2002). It is possible that similar mechanism can operate for surface-adsorbed Fe oxy(hydr)oxide as it is known for biogenic silica in marine sediments (Ward et al., 2022).

Therefore, some metals are capable of impacting the reactivity of phytoliths depending on whether they are incorporated into the mineral structure or remain on their surface.

4. CONCLUSIONS

In this study we assessed the factors that control multi-elemental composition of grass phytoliths, via measuring 56 major and trace elements in phytoliths extracted from grasses (poaecea) growing in Eastern European (Russian Plain) and Central and Southern Siberia. In the European part of Eurasia, different grass species from the same region exhibited very similar elemental composition of phytoliths. We observed rather insignificant impact of local climate, soil substrate and time of sampling during vegetative period on trace element concentration in European grass phytoliths. We also showed distinct differences in elemental composition of grasses sampled in European part of Russia and Siberia. In particular, phytoliths of European grasses from generally milder and wetter climate exhibited more than 10 times higher concentration of some labile elements (Ca, Sr and Se), compared to phytoliths from strongly continental climate of Siberia, whereas comparable concentrations of Li, B, Na, K, Mg, V, Zn, As, Mo, Ba and U were obtained for phytoliths from both locations. The phytoliths of Siberian grasses were strongly (x 10-100) enriched in lithogenic, low mobile elements and some heavy metals. We tentatively explain these differences by the differences in humidity regime and intensity of atmospheric silicate mineral dust deposits, linked to distance to the desert provinces of solid aerosols generation. In contrast, the local anthropogenic pollution and lithological aspect of parent rocks / soils played a sub-ordinary role. Considering all Eurasian grass phytoliths together, the concentration values of B, Na, Si, P, Sr, Mo, Ag, Cd, and Sb were comparable to those of upper crust. At the same time, grass phytoliths are generally poor in all lithogenic elements such as trivalent and tetravalent hydrolysates, divalent heavy metals, Ta, Bi, W, U. The upper crust-normalized composition of European grass phytoliths demonstrated

their sizable enrichment in macro and micronutrients and labile elements such as B, Na, Ca, Sr, Se, Mo, and U and strong depletion in lithogenic elements (Al, Ti, Y, Zr, Nb, Sn, Cs, REE, Hf, Pb, Ta, W, Tl, and Th) relative to the phytoliths of horsetail, fern, elm and larch. Overall, grasses exhibited distinctly different elemental composition compared to horsetail, fern, elm and larch.

A pairwise correlation analysis demonstrated two group of elements – (1) labile, soluble alkali, alkaline-earth metals and oxyanions and (2) lithogenic low mobile trivalent and tetravalent trace elements, heavy metals and toxicants. Despite significant, by 1 to 2 orders of magnitude difference in major element (Ca, Mg, Fe, Al) concentration in phytoliths from grass and those from other Si-concentrating plants studied previously (horsetail, fern, elm, larch), the dissolution rates of all phytoliths in circum-neutral aqueous solutions are identical within the experimental uncertainty. Our laboratory experiments confirm the use of phytoliths as environmental proxies and indicate that the preservation of phytoliths in soils is unrelated to phytolith elemental composition. Further work on mechanisms of trace element concentration by plant phytoliths via measuring element distribution coefficients between sap solution and precipitated amorphous silica should allow distinguishing different group of major and trace elements depending on their speciation in cellular fluids.

Acknowledgements

The European grass samples used in this study were collected by late Nina K. Kisileva. OP acknowledges a support from the TSU Development Programme 'Priority-2030'.

REFERENCES

Bartoli, F., 1981. Le cycle biogéochimique du silicium sur roches acides. Application à deux systèmes forestiers tempérés. Thèse de Doctorat, Université de Nancy I, 187 pp.

Bartoli, F., 1985. Crystallochemistry and surface properties of biogenic opal. Eur. J. Soil Sci. 36, 335–350.

Belton, D.J., Deschaume, O., Perry, C.C., 2012. An overview of the fundamentals of the chemistry of silica with relevance to biosilicification and technological advances. FEBS J. 279, 1710-1720.

Belton, D., Paine, G., Patwardhan, S.V., Perry, C.C., 2004. Towards an understanding of (bio)silicification: the role of amino acids and lysine oligomers in silicification. J. Mater. Chem. 14, 2231–2241.

Blecker, S.W., McCulley, R.L., Chadwick, O.A., Kelly, E.F., 2006. Biological cycling of silica across a grassland bioclimosequence. Global Biogeochem. Cycles 20, GB 3023. doi: 10.1029/2006GB002690.

Bujan, E., 2013. Elemental composition of phytoliths in modern plants (Ericaceae). Quat. Int. 287, 114–120.

Cabanes, 2020. Phytolith analysis in paleaocology and archaeology. In A. G. Henry (ed.), Handbook for the Analysis of Micro-Particles in Archaeological Samples, Interdisciplinary Contributions to Archaeology, https://doi.org/10.1007/978-3-030-42622-4_11.

Carnelli, A.L., Madella, M., Theurillat, J.P., Ammann, B., 2002. Aluminum in the opal silica reticule of phytoliths: A new tool in palaeoecological studies. Am. J. Bot. 89, 346–351.

Conley, D.J., 2002. Terrestrial ecosystems and the global biogeochemical silica cycle. Global Biogeochem. Cycles 16 (4), 1121. doi: 10.1029/2002GB001894.

Currie, H.A., Perry, C.C., 2007. Silica in plants: Biological, Biochemical and Chemical studies. Annals Botany 100, 1383-1389.

Delplace, G., Schreck, E., Pokrovsky, O.S., Zouiten, C., Darrozes, J., Viers, J., 2020. Accumulation of trace elements in phytoliths from reeds growing on mining environments in Southern Europe. Science Total Environ. 712, Art No 135595. https://doi.org/10.1016/j.scitotenv.2019.135595.

Derry, L.A., Kurtz, A.C., Ziegler, K., Chadwick, O.A., 2005. Biological control of terrestrial silica cycling and export fluxes to watersheds. Nature 433, 728-731.

Epstein, E., 1994. The anomaly of silicon in plant biology. Proc. Natl. Acad. Sci. U.S.A. 91, 11-17.

Epstein, E., 1999. Silicon. Annual Review of Plant Physiology and Plant Molecular Biology 50, 641–664.

Fraysse, F., Pokrovsky, O.S., Schott, J., Meunier, J.-D., 2006a. Surface properties, solubility and dissolution kinetics of bamboo phytoliths. Geochim. Cosmochim. Acta 70, 1939-1951.

Fraysse, F., Cantais, F., Pokrovsky, O.S., Schott, J., Meunier, J.D., 2006b. Aqueous reactivity of phytoliths and plant litter: physico-chemical constraints on terrestrial biogeochemical cycle of silicon. J. Geochem. Explorat. 88, 202-205.

Fraysse, F., Pokrovsky, O.S., Schott, J., Meunier, J.D., 2009. Surface chemistry and reactivity of plant phytoliths in aqueous solutions. Chemical Geology 258, 197-206.

Fraysse, F., Pokrovsky, O.S., Meunier J.D., 2010. Experimental study of terrestrial plant litter interaction with aqueous solutions. Geochim. Cosmochim. Acta 74, 70-84.

Gélabert, A., Pokrovsky, O.S., Schott, J., Feurtet-Mazel, A., 2018. Trace element (Cr, Mo, W, As, Sb, Al, Ga, Ge) interaction with marine and freshwater diatoms: a physico-chemical approach. Chemical Geology, 494, 117-126. doi:10.1016/j.chemgeo.2018.07.025.

Guerriero, G., Hausman, J.-F., Legay, S., 2016. Silicon and plant extracellular matrix. Front. Plant Sci. 7, 463, doi: 10.3389/fpls.2016.0043.

Hart, D., 2001. Elements occluded within phytoliths. In J. D. Meunier, & F. Colin (Eds.), Phytoliths: Applications in Earth Sciences and Human History (pp. 313-316). A. A. Balkema.

Heřmanská, M., Voigt, M.J., Marieni, C., Declercq, J., Oelkers, E.H., 2022. A comprehensive and internally consistent mineral dissolution rate database: Part I: Primary silicate minerals and glasses. Chemical Geology, 597, Art No 120807, https://doi.org/10.1016/j.chemgeo.2022.120807.

Hodson, M.J., 2015. The Development of Phytoliths in Plants and its Influence on their Chemistry and Isotopic Composition. Implications for Palaeoecology and Archaeology. J. Archaeological Sci. 68, 62-69. doi: 10.1016/j.jas.2015.09.002.

Hodson, M.J., 2016. The development of phytoliths in plants and its influence on their chemistry and isotopic composition. Implications for palaeoecology and archaeology. J. Archaeol. Sci. 68, 62–69.

Hodson, M.J., 2018. Phytoliths in archaeology: chemical aspects. In C. Smith (ed.), Encyclopedia of Global Archaeology, https://doi.org/10.1007/978-3-319-51726-1_3250-1.

Hodson, M.J., Sangster, D.E., 1999. Aluminium/silicon interactions in conifers. J. Inorg. Biochemistry 76, 89-98.

Hussain, B., Riaz, L., Li, K., Hayat, K., Akbar, N., Hadeed, M.Z., Zhu, B., Pu, S., 2023. Abiogenic silicon: Interaction with potentially toxic elements and its ecological significance in soil and plant systems. Environmental Pollution 338, Ar No 122689, https://doi.org/10.1016/j.envpol.2023.122689.

Jones, R.L., Beavers, A.H., 1963. Some mineralogical and chemical properties of plant opal. Soil Science 96, 375–379.

Jones, L., Milne, A., Sanders, J., 1966. Tabashir: An opal of plant origin. Science, 151, 464–466.

Kaczorek, D., Puppe, D., Busse, J., Sommer, M., 2019. Effects of phytolith distribution and characteristics on extractable silicon fractions in soils under different vegetation – An exploratory study of loess. Geoderma 356, Art No 113917.

Kameník, J.; Mizera, J.; Řanda, Z., 2013. Chemical composition of plant silica phytoliths. Environ. Chem. Lett., 11, 189–195.

Keller C., Rizwan M., Davidian J.-C., Pokrovsky O.S., Bovet N., Chaurand P., Meunier J.-D., 2015. Effect of silicon on wheat seedlings (*Triticum turgidum* L.) grown in hydroponics and exposed to 0 to 30 µM Cu. Planta, 241, 847-860.

Krickov, I.V., Lim, A.G., Shevchenko, V.P., Vorobyev S.N., Pokrovsky O.S., 2022. Low molecular weight and colloidal major and trace elements in snow of western Siberia. Chemical Geology, 610, Art No 121090. https://doi.org/10.1016/j.chemgeo.2022.121090.

Kučera, J., Mizera, J., Řanda, Z., Vávrová, M., 2007. Pollution of agricultural crops with lanthanides, thorium and uranium studied by instrumental and radiochemical neutron activation analysis. J. Radioanal. Nucl. Chem. 271, 581–587.

Li, Z., Song, Z., Li, B., 2013. The production and accumulation of phytolith-occluded carbon in Baiyangdian reed wetland of China. Applied Geochem. 37, 117-124, https://doi.org/10.1016/j.apgeochem.2013.07.012.

Li, Z., Song, Z., Cornelis, J.T., 2014. Impact of rice cultivar and organ on elemental composition of phytoliths and the release of bio-available silicon. Front. Plant Sci., Sec. Functional Plant Ecology, 5, Art No 529, doi: 10.3389/fpls.2014.00529.

Li, R., Wen, M., Tao, X., Liu, Y., Li, C., 2020. Advance of study on chemical composition of phytolith. Quaternary Sci. 40(1), 283–293. https://doi.org/10.11928/j.issn.1001-7410.2020.01.26.

Liang, Y., Nikolic, M., Bélanger, R., Gong, H., Song, A., 2015. Silicon in agriculture. Springer, Netherlands.

679 Lim, A., Pokrovsky, O.S., Cornu, S., Meunier, J.-D., 2023. Release of labile Si from forest and
680 agricultural soils. Catena 229, Art No 107211.
681 Liu, H., Meunier, J.D., Grauby, O., Labille, J., Alexandre, A., Barboni, D., 2023. Dissolution
682 does not affect grass phytolith assemblages. Pal. Pal. Pal. 610, Art No 111345.
683 Liu, L., Jie, D., Liu, H., Gao, G., Gao, Z., Li, D., Li, N., Guo, J., Qiao, Z., 2016a. Assessing the
684 importance of environmental factors to phytoliths of *Phragmites communis* in north-
685 eastern China. Ecol. Indic., 69, 500–507.
686 Liu, H.Y., Jie, D.M., Liu, L.D., Li, N.N., Wang, T., Qiao, Z.H., 2016b. The shape factors of
687 phytoliths in selected plants from the Changbai Mountains and their implications. Rev.
688 Palaeobot. Palynol. 2016, 226, 44–53.
689 Liu, L., Song, Z., Li, Q., Ellam, R.M., Tang, J., Wang, Y., Sarkar, B., Wang, H., 2022.
690 Accumulation and partitioning of toxic trace metal(loids) in phytoliths of wheat grown in
691 a multi-element contaminated soil. Environ. Poll. 294, Art No 118645.
692 Liu, L., Song, Z., Tang, J., Li, Q., Sarkar, B., Ellam, R.M., Wang, Y., Zhu, X., Bolan, N.,
693 Wang, H., 2023. New insight into the mechanisms of preferential encapsulation of
694 metal(loid)s by wheat phytoliths under silicon nanoparticle amendment. Sci. Total
695 Environ. 875, Art No 162680, https://doi.org/10.1016/j.scitotenv.2023.162680.
696 Meunier, J.-D., Colin, F., Alarcon, C., 1999. Biogenic silica storage in soils. Geology 27,
697 835-838.
698 Meunier, J.D., Cornu, S., Keller, C., Barboni, D., 2022. The role of silicon in the supply of
699 terrestrial ecosystem services. Environ. Chem. Lett. 20, 2109-2121.
700 https://doi.org/10.1007/s10311-021-01376-8.
701 Montes-Botella C., 2001. Condictionamientos Ambientales de Erica andevalensis Cabezudo
702 and Rivera. Respuestra frente a Metales Pesados. Ph.D. thesis. University Polytechnic of
703 Madrid. Spain.
704 Nawaz, M.A., Zakharenko, A.M., Zemchenko, I.V., Haider, M.S., Ali, M.A. et al., 2019.
705 Phytolith formation in plants: from soil to cell. Plants 8, Art No 249, doi:
706 10.3390/plants8080249.
707 Neethirajan, S., Gordon, R., Wang, L., 2009. Potential of silica bodies (phytoliths) for
708 nanotechnology. Trends Biotechnol. 27(8), 461-467.
709 Nguyen, A.T.Q., Nguyen, A.M., Pham, N.T.T., Nguyen, H.X., Dang, Q.T., Tran, T.M.,
710 Nguyen, A.D., Tran, P.D., Nguyen, M.N., 2021. CO_2 can decrease the dissolution rate of
711 ashed phytoliths. Geoderma 385, Art No 114835.
712 Nguyen, N.M., Dultz S., Picardal, F., Bui, T.K.A., Pham, Q.V., Schieber, J., 2015. Release of
713 potassium accompanying the dissolution of rice straw phytoliths. Chemosphere 119, 371-
714 376.
715 Nguyen, N.T., Nguyen, A.M., McNamara, M., Dultz, S., Mehard, A. et al., 2019. Encapsulation
716 of lead in rice phytoliths as a possible pollutant source in paddy soils. Environ. Exp. Bot.,
717 162, 58-66.
718 Oelkers, E.H., 2001. General kinetic description of multi-oxide silicate mineral and glass
719 dissolution. Geochim. Cosmochim. Acta 65, 3703-3719.
720 Oelkers, E.H., Golubev, S.V., Chairat, C., Pokrovsky, O.S., Schott, J., 2009. The surface
721 chemistry of multi-oxide silicates. Geochim. Cosmochim. Acta 73, 4617-4634.
722 Parr, J.F., Lentfer, C.J., Boyd, W.E., 2001. A comparative analysis of wet and dry ashing
723 techniques for the extraction of phytoliths from plant material. J. Arch. Sci. 28, 875-
724 886.
725 Parr, J.F., Dolic, V., Lancaster, G., Boyd, W.E., 2001. A microwave digestion for the
726 extraction of phytoliths from herbarium specimens. Rev. Palaeobotany and Palynologie
727 116, 203-212.
728 Parr, J.F., Sullivan, L.A., 2005. Soil carbon sequestration in phytoliths. Soil Biol. Biochem.

37(1), 117-124. https://doi.org/10.1016/j.soilbio.2004.06.013.
Perry, C.C., Fraser, M.A., 1991. Silica deposition and ultrastructure in the cell wall of Equisetum arvense: the importance of cell wall structures and flow control in biosilicification? Phil. Trans. Royal Soc. London B 334, 149–157.
Perry, C.C., Keeling-Tucker, T., 1998. Aspects of the bioinorganic chemistry of silicon in conjunction with the biometals calcium, iron and aluminium. J. Inorg. Biochem. 69, 181-191.
Perry, C.C., Keeling-Tucker, T., 2000a. Biosilicification: the role of the organic matrix in structure control. J. Biol. Inorg. Chem. 5, 537-550.
Perry, C.C., Keeling-Tucker, R., 2000b. Model studies of the precipitation of silica in the presence of aluminium; implications for biology and industry. J. Inorgan. Biochem. 78, 331-339.
Piperno, D.R., 1988. Phytolith. An archaeological and geological perspective. Academic Press, London, 280 pp.
Rizwan, M., Meunier, J.-D., Davidian, J.-C., Pokrovsky, O.S., Bovet, N., Keller, C., 2016. Silicon alleviates Cd stress of wheat seedlings (*Triticum turgidum* L. cv. Claudio) grown in hydroponics. Environmental Science Pollution Research, 23, 1414–1427, doi:10.1007/s11356-015-5351-4.
Rossini, S., Valdés, B., Leidic, E.O., 2009. Accumulation and in vivo tissue distribution of pollutant elements in Erica andevalensis. Sci. Total. Environ. 407(1), 1929-1936.
Rossini, S., Mingorance, M.D., Leidi, E.O., 2011. Effects of silicon on copper toxicity in Erica andevalensis Cabezudo and Rivera: a potential species to remediate contaminated soils. J. Environ. Monitoring 13, 591-596.
Rudnick, R.L., Gao, S., 2004. V. 3, Chapter 3.01: Composition of the Continental Crust. In: Treatise On Geochemistry, Elsevier, Amsterdam.
Santos, G.M., Alexandre, A., Southon, J.R., Treseder, K.K., Corbineau, R., Reyerson, P.E., 2012. Possible source of ancient carbon in phytolith concentrates from harvested grasses. Biogeosciences, 9, 1873–1884. doi:10.5194/bg-9-1873-2012.
Sapei, L., Gierlinger, N., Hartmann, J., Nöske, R., Strauch, P., Paris, O., 2007. Structural and analytical studies of silica accumulations in Equisetum hyemale. Anal. Bioanal. Chem. 389, 1249-1257.
Sarret, G., Schreck, E., Findling, N., Daval, D., Viers, J., Delplace, G., Pokrovsky, O.S., 2022. Zn chemical status in plant phytoliths: impact of calcination and (paleo) environmental implications. Science Total Environment, 852, Art No 158460. https://doi.org/10.1016/j.scitotenv.2022.158460.
Schaller, J., Puppe, D., Kaczorek, D., Ellerbrock, R., Sommer, M., 2021. Silicon cycling in soils revisited. Plants 10, Art No 295. https://doi.org/ 10.3390/plants10020295
Shevchenko, V.P., Pokrovsky, O.S., Vorobyev, S.N., Krickov, I.V., Manasypov, R.M., Politova, N.V., Kopysov, S.G., Dara, O.M., Auda, Y., Shirokova, L.S., et al., 2017. Impact of snow deposition on major and trace element concentrations and elementary fluxes in surface waters of the Western Siberian Lowland across a 1700 km latitudinal gradient. Hydrol. Earth Syst. Sci., 21, 5725–5746.
Shevchenko, V.P., Vorobyev, S.N., Krickov, I.V., Boev, A.G., Lim, A.G., Novigatsky, A.N., Starodymova, D.P., Pokrovsky, O.S., 2020. Insoluble particles in the snowpack of the Ob river basin (Western Siberia) a 2800 km submeridional profile. Atmosphere, 11, Art No 1184.
Song, Z., McGrouther, K., Wang, H., 2016. Occurrence, turnover and carbon sequestration potential of phytoliths in terrestrial ecosystems. Earth-Sci. Rev. 158, 19-30.

Tan, S., Li, R., Vachula, R.S., Tao, X., Wen, M., Liu, Y., et al., 2022. Electron probe microanalysis of the elemental composition of phytoliths from woody bamboo species. PLoS ONE 17(7), Art No e0270842. https://doi.org/10.1371/journal.pone.0270842.

Tran, C.T., Mai, N.T., Nguyen, V.T., Nguyen, H.X., Meharg, A., Carey, M. et al., 2018. Phytolith-associated potassium in fern : Characterization, dissolution properties and implications for slash-and-burn agriculture. Soil Use Manage. 34(1), 28-36.

Tran, T.T.T., Nguyen, T.T., Nguyen, V.T., Huynh, H.T.H., Nguyen, T.T.H., Nguyen, M.N., 2019. Copper encapsulated in grass-derived phytoliths: Characterization, dissolution properties and the relation of content to soil properties. J. Environ. Manag. 249, 109423.

Turnau, K., Henriques, F.S., Anielska, T., Renker, C., Buscot, F., 2007. Metal uptake and detoxification mechanisms in *Erica andevalensis* growing in a pyrite mine tailing. Environ. Experimental Botany 61, 117-123.

Van Cappellen, P., Dixit, S., van Beusekom, J., 2002. Biogenic silica dissolution in the oceans: reconciling experimental and field-based dissolution rates. Glob. Biogeochem. Cycles 16(4), Art No 1075, doi:10.1029/2001GB001431.

Ward, J., Hendry, K., Arndt, S., Faust, J., Freitas, F., Henley, S. F., Krause, J., Maerz, C., Ng, H. C., Pickering, R., 2022. Stable silicon isotopes uncover a mineralogical control on the benthic silicon cycle in the Arctic Barents Sea. Geochim. Cosmochim. Acta 329, 206–230, https://doi.org/10.1016/j.gca.2022.05.005.

WRB, 2022. USS Working Group: World Reference Base for Soil Resources. International soil classification system for naming soils and creating legends for soil maps. 4th edition. International Union of Soil Sciences (IUSS), Vienna, Austria.

Wyttenbach, A., Tobler, L., 2002. Soil contamination in plant samples and in botanical reference materials: Signature, quantification and consequences. J. Radioanal. Nucl. Chem. 254, 165–174.

Table 1. List of studied plant phytoliths, sampling location (see Fig. 1 for the map), landscape, climate and soil parameters. MAP and MAAT are mean annual precipitation and air temperature, respectively. Soil type is defined according to WRB (2022). Climate data are from http://climatebase.ru/

1A: European grasses

N°	Name	Typical environment	Sampling date	Location	MAP, mm y^{-1}	MAAT, °C	Soil type (WRB 2022)	Soil parent material
E1	*Calamagrostis epigejos*	Temperate coniferous-deciduous forests	06/14/1998	Bor, Russia	630	4.4	Albic Glossic Retisol	Clay glacial till
E2	*Calamagrostis epigejos*	Temperate coniferous-deciduous forests	07/14/2000	Malinki region, Russia	630	4.4	Albic Retisol	Clay glacial till
E3	*Calamagrostis epigejos*	Temperate coniferous-deciduous forests	06/30/2000	Yaroslavl region, Russia	687	4.2	Albic Stagnic Retisol	Boulder and pebble loamy glacial tills
E4	*Phragmites communis*	Temperate coniferous-deciduous forests	07/17/1998	West Dvina, Russia	692	5.2	Mollic Gleysol	Thin thickness fluvioglacial deposits on clay tills
E5	*Calamagrostis epigejos*	Temperate coniferous-deciduous forests	08/02/1998	Bor, Russia	630	4,5	Albic Glossic Retisol	Clay glacial till
E6	*Calamagrostis epigejos*	Desert steppes	08/03/2000	Kalmykia region, Russia	349	9.5	Calcic Kashtanozem	Loess deposits
E7	*Glyceria maxima*	Wetlands in Europe	07/17/1998	West Dvina, Russia	692	5.2	Subaquatic Gleysol	Coastal lake deposits
E8	*Anthoxanthum odoratum*	Acidic grassland in Eurasia	07/17/1998	West Dvina, Russia	692	5.2	Albic Retisol (Aric)	Thin fluvioglacial deposits on clay tills
E9	*Calamagrostis epigejos*	Temperate continental steppe	07/06/2003	Saratov region, Russia	458	6.5	Calcic Chernozem	Saline clays overlain by thin loess-like loams
E10	*Calamagrostis epigejos*	Temperate coniferous-deciduous forests	06/09/2000	Yaroslavl region, Russia	687	4.2	Albic Stagnic Retisol	Boulder and pebble loamy glacial tills
E11	*Calamagrostis arundinacea*	Temperate coniferous-deciduous forests	07/17/1998	West Dvina, Russia	692	5.2	Albic Retisol (Epiarenic, Endoclayic)	Fluvioglacial sands on clay tills
E12	*Calamagrostis epigejos*	Temperate coniferous-deciduous forests	10/03/1998	Bor, Russia	630	4.4	Albic Glossic Retisol	Clay glacial till

816 **Table 1 B: Siberian grasses**

N°	Name	Typical environment	Sampling date	Location	MAP, mm	MAAT, °C	Soil type (WRB 2022)	Soil parent material
S1	*P. communis*	Floodplain in a sharply continental climate	08/5/1974	Yakutia, 7 km SW from Yakutsk	216	–9.0	Dystric Fluvisol	Alluvial deposits
S2	*C. epigejos*	Dry steppe in continental climate	08/12/1927	Northern Baraba, village Mitrofanovka	333	1.2	Calcic Mollic Solonetz	Layered loess-like silt and loam deposits
S3	*C. arundinacea*	Barrier-rain temperate continental forests	08/29/1956	Kemerskaya region, Leninsk-Kuznetsky district	673	2.0	Albic Luvisol (Ochric)	Loess-like cover clay deposits
S4	*G. maxima*	Continental deciduous forests	07/16/1969	Tomskaya region, Zyryansky distr., d. Cherdaty, lake Charochkino	520	1.0	Greyzemic Phaeozem	Loess-like loam deposits
S5	*C. arundinacea*	Continental light coniferous forests	08/25/1959	Krasnoyarsk region, Natl. Park Stolby, riparian zone of spring	483	1.2	Mollic Gleysol	Alluvial deposits
S6	*A. odoratum*	Mountain continental taiga	08/10/1936	Krasnoyarsk region, watershed divide of Kazyr and Kizir	600	–1.0	Skeletic Cambisol (Ochric)	Colluvium felsic metamorphic and igneous rocks
S7	*G. maxima*	Barrier-rain temperate continental forests	07/8/1928	Altai, villages Troitskaya and Kebezen	778	1.1	Albic Luivisol	Loess-like clays on colluvium of shale and sandstone
S8	*C. epigejos*	Continental steppe	07/23/1931	NW Altai, Rubtsovsky distr., d. Berezovka and Ermelikha	331	2.7	Calcic Chernozem	Carbonate loess
S9	*C. epigejos*	Continental forest-steppe	07/27/1939	Krasnoyarsk region, Rybinsk district, d. Krasnoyarovka	450	–0.4	Luvic Phaeozem (Albic)	Clayey and heavy loamy gravelly colluvial deposits
S10	*G. maxima*	Continental lowland southern taiga	07/27/1970	Tomskaya region, Kolpashevsky dist., Ob's River floodplain, d. Pavlovka	489	–0.4	Orthofluvic Fluvisol (Aric)	Alluvial silt-clay deposits
S11	*A. odoratum*	Continental light coniferous and small-leaved forests	07/14/1966	Tomskaya region, Tomsk, d. Anikino	544	0.9	Luvic Phaeozem (Albic)	Cover loess-like loams.
S12	*A. odoratum*	Sharply continental mountain boreal taiga	08/9/1959	Buryatia, Natl. Park Barguzinsky, rivers Talamysh and Malaya	450	–2.0	Leptic Regosol (Ochric)	Colluvium from felsic metamorphic and igneous rocks and shales
S13	*G. maxima*	Continental steppe	07/8/1969	Omskaya region, Nazyvaevsky dist., d. Iskra	398	2.0	Gleyic Chernozem	Lacustrine alluvial deposits
S14	*P. communis*	Continental mountain boreal taiga	07/29/1975	Tuva, Piy-Khemsky dist, Uyukski ridge, d. Saigara	305	–1.4	Skeletic Regosol (Ochric)	Shale colluvium
S15	*P. communis*	Continental lowland southern taiga	08/1/1958	Tomskaya region, Molchanovsky dist., pos. Suiga	470	0.4	Brunic Arenosol (Aric)	Aeolian sand deposits
S16	*A. odoratum*	Mountain forest-tundra	07/22/1975	Tuva, Todzhinsky dist., lake Karabalyk	350	–4.4	Brunic Regosol	Sandy colluvium of basic metamorphic and igneous rocks and sandstones
S17	*C. arundinacea*	Continental light coniferous and small-leaved forests	07/28/1972	Novosibirsk region, d. Kisilevka	485	1.3	Luvic Greyzemic Phaeozem	Loess-like clays
S18	*C. epigejos*	Continental forest-tundra in a zone of discontinuous permafrost	08/2/2014	Khanymey station of INTERACT, Nojabrsk region	520	–3.4	Histic Fluvisol	Lake sediments

817

818 **Table 2**. Mass content of the phytoliths in the grass biomass and total Si concentration in

819 phytoliths

820 **A:** Phytoliths of grasses from Eastern Europe

Sample	Phytoliths content in biomass, %	% mass Si in phytoliths
E1 *C. epigejos*	2.0	38,9
2. *C. epigejos*	4.6	42,6
3. *C. epigejos*	0.9	35,3
4. *P. communis*	0.9	40,3
5. *C. epigejos*	1.8	39,2
6. *C. epigejos*	3.4	39,5
7. *G. maxima*	0.9	37,8
9. *C. epigejos*	2.9	42,0
10. *C.epigejos*	3.4	35,8
11. *C. arundinacea*	6.7	39,8

821

822 B: Phytoliths of grasses from Siberia

Sample N°	Phytoliths content in biomass, %	% mass Si
S1	1.15	38.8
S2	1.88	42.6
S3	1.33	33.0
S4	1.84	24.8
S5	2.45	32.2
S6	0.16	32.8
S7	2.40	32.3
S8	2.60	32.1
S9	2.62	50.8
S10	1.11	32.7
S11	0.70	15.6
S12	1.19	22.9
S13	1.82	57.3
S14	1.23	34.6
S15	0.51	29.3
S16	0.52	23.0
S17	3.09	28.5
S18	0.44	43.3

823

824 **Table 3.** Mean elementary composition (ppm dry weight) of grass phytoliths (n = 27) extracted
825 from *C. epigejos*, *C. arundinacea*, *G. maxima*, *P. communis*, and *A. odoratum* which were
826 sampled in Eastern Europe and Siberia.
827

Li	2.4
B	18
Na	3800
Mg	4300
Al	1900
Si	356000
P	215
K	3800
Ca	24000
Sc	0.46
Ti	150
V	2.8
Cr	1.9
Mn	114
Fe	680
Co	0.2
Ni	1.0
Cu	7.5
Zn	21
Ga	3.7
Ge	0.11
As	0.54
Se	1.7
Rb	13
Sr	390
Y	0.43
Zr	2.7
Nb	0.40
Mo	0.60
Ag	0.088
Cd	0.067
Sn	0.63
Sb	0.17
Cs	0.30
Ba	45
La	0.66
Ce	1.4
Pr	0.16
Nd	0.60
Sm	0.12
Eu	0.028

Tb	0.016
Gd	0.093
Dy	0.080
Ho	0.016
Er	0.048
Tm	0.0073
Yb	0.051
Lu	0.0074
Hf	0.081
Ta	0.037
W	0.082
Tl	0.055
Pb	1.3
Bi	0.0004
Th	0.17
U	0.20

844 **Table 4.** Dissolution rates of *C. epigejos* phytoliths at 25°C in 0.01M NaCl and pH = 4.5 ± 0.1.

845

Sample	R_{Si}, mol g^{-1} d^{-1}
C. epigeios E1	$(3.70\pm0.25)\times10^{-5}$
C. epigeios E2	$(5.76\pm0.30)\times10^{-5}$
C. epigeios E3	$(3.29\pm0.20)\times10^{-5}$
C. epigeios E5	$(5.55\pm0.25)\times10^{-5}$
C. epigeios E9	$(6.58\pm0.40)\times10^{-5}$

846

847

848

849

850

851

852

853

854

855

856 **Fig. 1**. A map of sampling sites for grasses used for phytolith extraction.

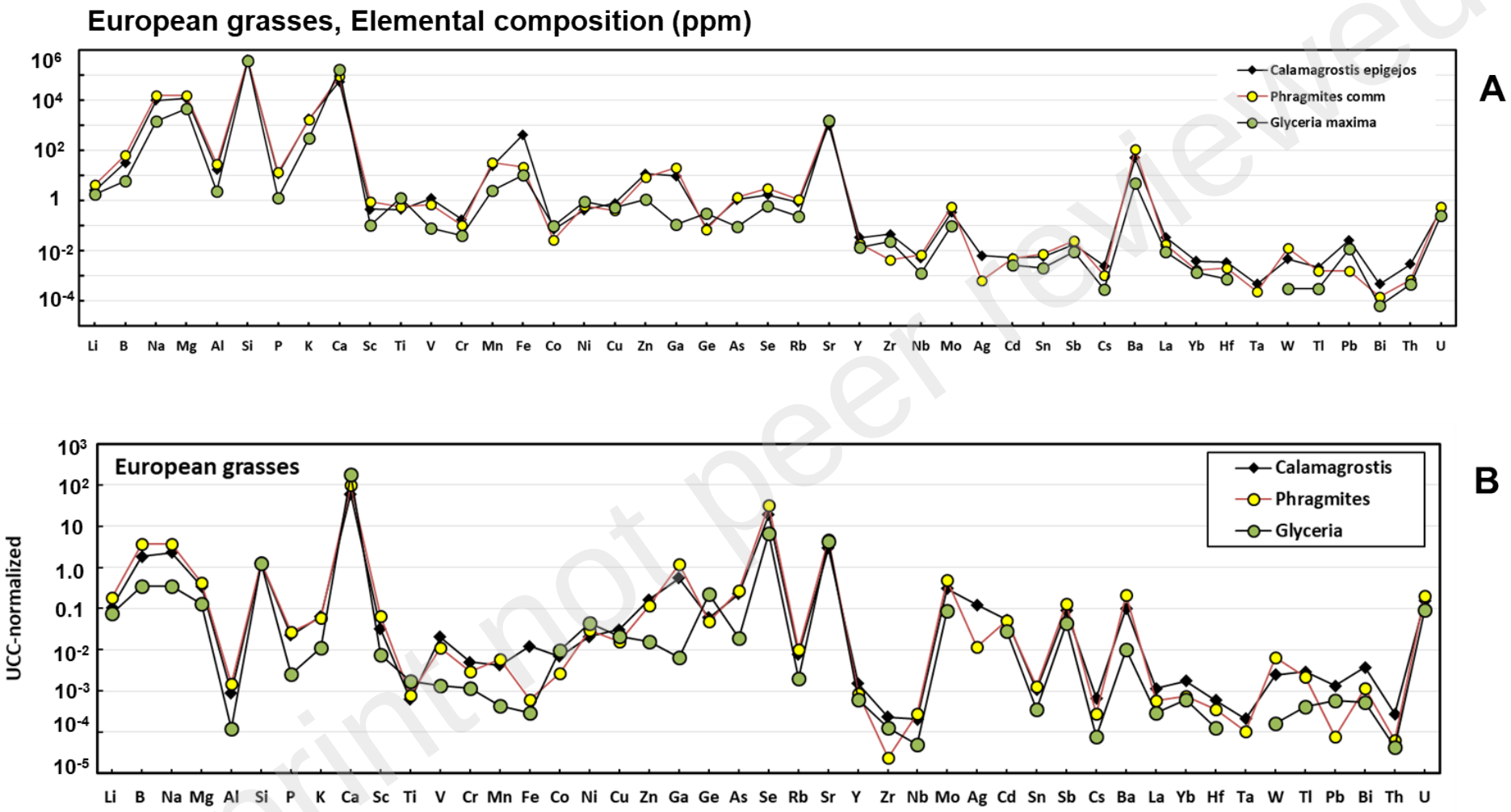

Figure 2. Mean elemental composition of phytoliths from European grasses (**A**) and UCC-normalized pattern of major and trace elements (**B**).

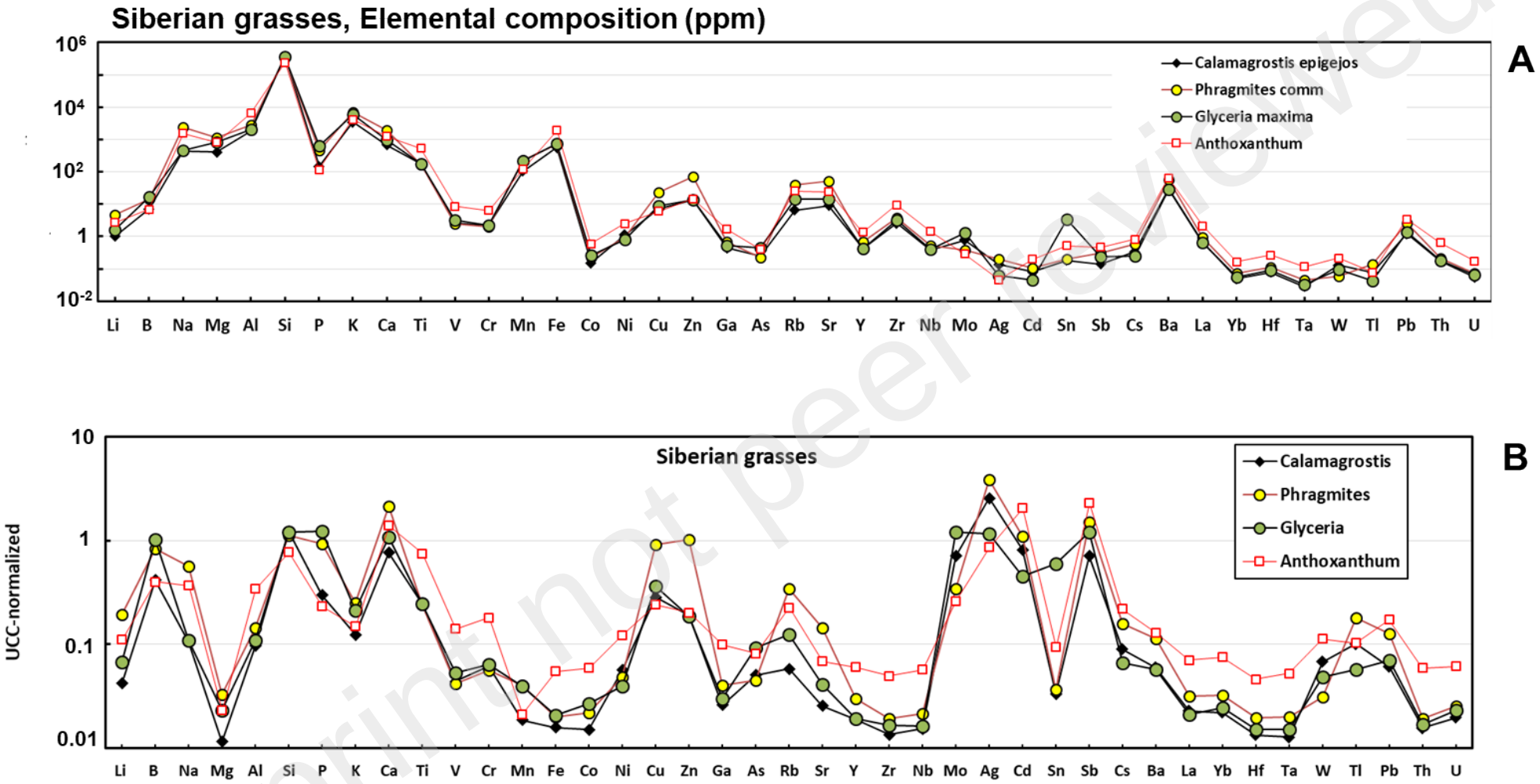

Figure 3. Mean elemental composition of phytoliths from Siberian grasses (**A**) and UCC-normalized pattern of major and trace elements (**B**).

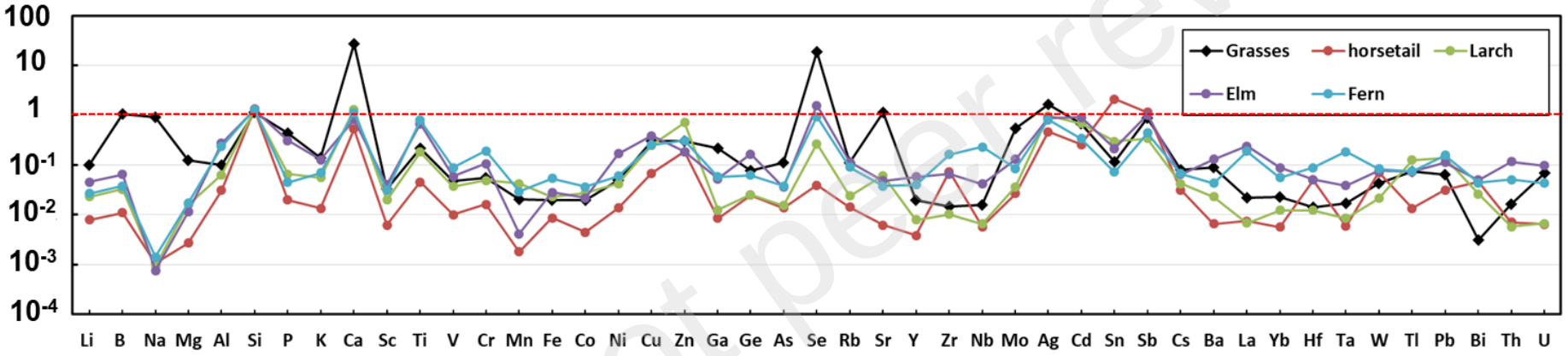

Figure 4. Upper Continental Crust-normalized pattern of grass phytolith (mean of European and Siberian) elemental composition compare to that of other Si-concentrating plants (horsetail, fern, larch and elm).

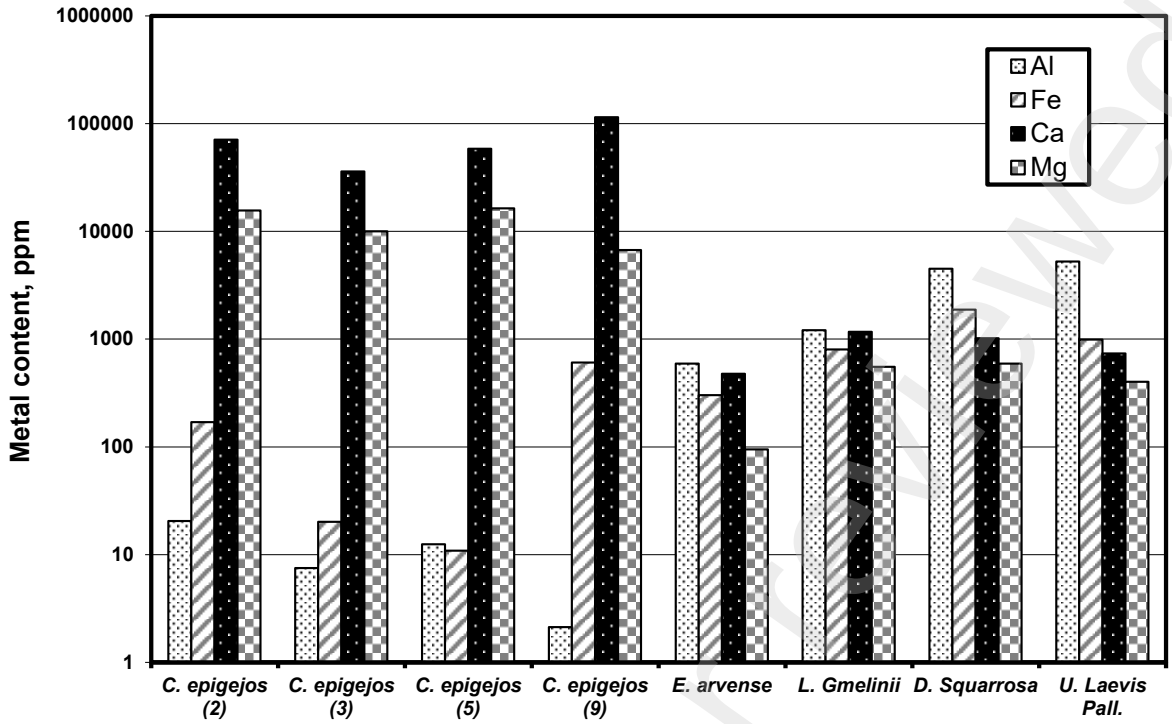

Figure 5. Al, Fe, Ca and Mg contents (ppm) in phytoliths used in present (*C.epigejos*, samples 2, 3, 5 and 9) and previous study (*E. arvense*, *L. gmelinii*, *D. squarrosa* and *U. Laevis* Pall.; Fraysse et al., 2009) of dissolution kinetics.

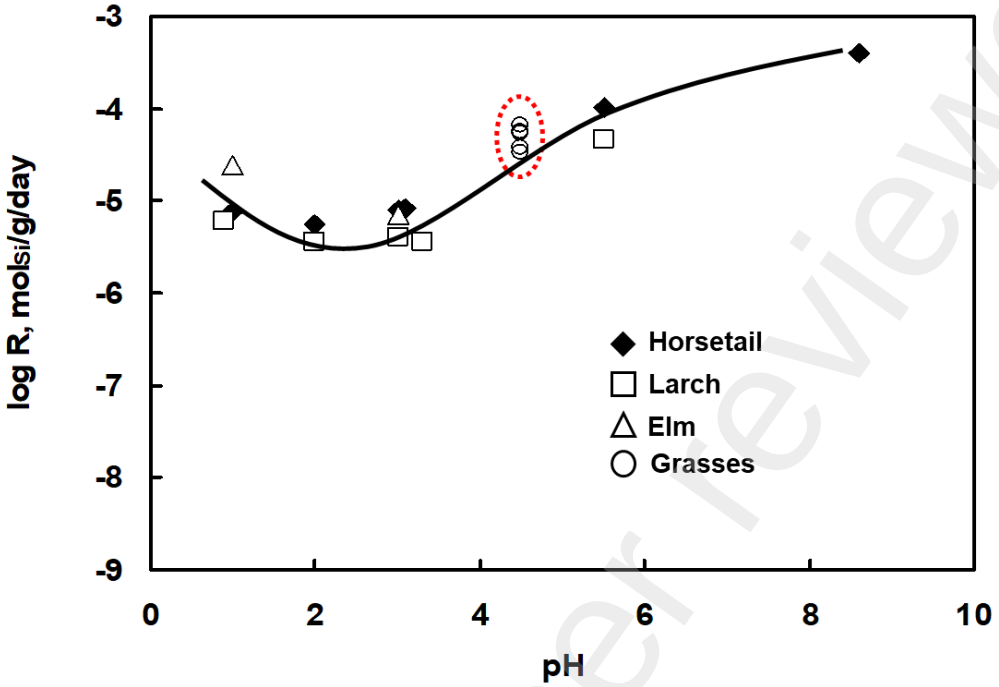

Figure 6. Dissolution rates of *Calamagrostis epigejos* (open circles, encircled by red contour) phytoliths at 25°C as a function of pH, compared to phytoliths from larch (squares), horsetail (solid diamonds), elm (triangles). The solid line is generic phytolith rate dependence on pH, based on previous studies with bamboo phytoliths (Fraysse et al., 2009).